

TRENDS AND PATTERNS IN U.S. DAILY TOTAL AND EXTREME PRECIPITATION SINCE 1893

John Christy
The University of Alabama in Huntsville

Ross McKittrick
University of Guelph
Guelph Ontario Canada
Ross.mckittrick@uoguelph.ca

April 14, 2026

Abstract

We present a newly-constructed set of U.S. daily precipitation observations at 377 locations in nine CONUS regions. Our data end in 2025 and extend back to at least 1893 and in some places as far back as 1872, making this the longest completely continuous daily rainfall record ever assembled for the CONUS. We examine seven metrics covering annual total, skewness and extreme values. We conduct trend evaluations over the entire sample and over the post-1958 and post-1980 subsamples. Indications of positive trends are mainly in the eastern half of CONUS. Upward trends in annual total precipitation are found in the Mid-West, Northeast and Gulf South but they do not persist in the post-1980 subsample. Annual maximum precipitation has trended up in the Southeast and Atlantic South region post-1980 while summertime precipitation in the Intermountain region has trended down since 1958. We also undertake Generalized Extreme Value modeling of the influence of climate on annual block maxima. Attributable trends in maximum precipitation are found at individual locations and at regional levels (Northeast, Atlantic South and Gulf South) on long time scales, although not post-1958. We also present a panel regression (pooled regional cross-section and time series) analysis of CONUS-wide annual maxima. We find a significant role for temperature, but only in the east, and a significant role for ENSO. Overall, we find precipitation is a complex phenomenon that varies regionally and by time interval: also average and extreme rainfall metrics do not necessarily share trends. Weather-sensitive planning operations such as agriculture and flood management would thus benefit most from local analysis of the longest possible data records.

Significance statement

We assembled the longest ever continuous, complete, quality-controlled record of daily precipitation for 377 locations across the continental US. We apply trend analyses over multiple time scales on eight precipitation metrics covering total, extreme and clustering phenomena. We also undertake nonstationary Generalized Extreme Value modeling and panel regression to test whether changes in annual maxima can be attributed to climatic factors. In line with other studies we find positive trends tend to be in eastern regions, although the west-east contrast attenuates after 1980. Annual maxima are sensitive to El Niño events but global warming plays an insignificant role. The extent of regional and temporal heterogeneity argues against trying to make continental-scale generalizations regarding changes in average or extreme precipitation.

1 INTRODUCTION

With rising atmospheric concentrations of infrared-active (greenhouse) gasses there is concern that various precipitation-related phenomena may be changing in sufficiently harmful ways as to require changes to disaster management infrastructure (Kunkel et al. 2019). More generally, changes in seasonal and annual rainfall can have economic impacts such as through agricultural productivity. Some data assessments have offered generalized conclusions about current trends. For instance the *Fifth National Climate Assessment* (NCA5, USGCRP 2023) reported that the frequency and intensity of heavy precipitation events scales with the global warming level (Marvel et al. 2023 p. 2-24) and that since 1958, the total precipitation falling in the heaviest 1% of daily precipitation events has increased between 37 and 60% in the eastern CONUS (Fig 2.8, Ch. 2 NCA5, Marvel et al. 2023). Other studies, however, have found spatial and temporal heterogeneity limits the generalizations that can be made at the continental and even regional scale (Kunkel et al. 2019, van der Wiel et al. 2016, Jorgensen and Nielsen-Gammon 2024).

The starting point for understanding the potential magnitude of extreme local weather is an accurate record of what has happened historically over the longest possible interval. Here we present a new CONUS-wide archive of daily rainfall records from 377 monitoring sites that is twice as long as indicated in NCA5 and extends further back in time than any previous rainfall data set. The process of constructing this data set revealed many flaws and omissions in currently-available rainfall archives. Once the data are collected there is an essentially unlimited number of metrics one might examine to discover changes over time (e.g., 1-day, 2-day, 3-day ... totals, 1%, 2%, 3% ... heaviest events, seasonal totals, annual totals, changes in skewness, changes in variance, etc.). We shall focus on a few that are traditional and thus comparable with earlier studies and others that have been proposed as being related to the overall warming of the planet.

There are also many statistical modeling techniques available. We begin by fitting a linear trend over, for each metric in each location and region, the entire daily sample back to at least 1893 and ending in 2025 and subsamples beginning in 1958 and 1980. Jorgensen and Nielsen-Gammon (2024) caution that a linear trend over the entire post-1900 interval may not be informative as to current changes. Examining different time scales thus guards against drawing conclusions based on, for instance, a post-1958 trend that apparently rationalizes a hypothesis which is then contradicted if the trend changes sign post-1980. We assess trend significance using autocorrelation-consistent standard errors drawn from the econometrics literature. We also conduct an attribution analysis by fitting a Generalized Extreme Value model of annual maximum precipitation allowing the location parameter to vary linearly with the global average temperature anomaly, the El Niño Southern Oscillation (ENSO) index and an indicator of known changes to measurement equipment. Finally, we pool the regional averages and present a national panel regression to see what can be said about CONUS-wide attributable changes in maximum precipitation. Since there are many thousands of regressions involved the results are summarized in a very compressed format, but all individual results are available in the Supplement.

We focus on daily total precipitation so we are unable to discuss rainfall events on the hourly time scale. We primarily look at metrics on the annual scale but we do include summertime total rainfall. Our analysis comprises over 9,000 regressions so to make the presentation of results manageable we will primarily report regional and continental scale summaries.

2 DATA AND METRICS

2.1 DATA SOURCES AND DESCRIPTION

Analyzing a metric as erratic as daily precipitation requires observations that are consistent, long-term and complete to capture as much of the natural character of its statistical properties as possible. Here we expand and update the more limited dataset analyzed in McKittrick and Christy 2019 to regions throughout the CONUS. As in McKittrick and Christy 2019, the datasets constructed here are different from nearly all others as they are truly complete, containing no missing entries for the time periods examined. Those values that were determined to be truly missing in the original forms (see below) were in-filled by a measurement from a nearby station.

Spatial and temporal coverage

Altogether we present records from 377 U.S. locations grouped into nine regions, each extending back at least to 1893. The regions are (codes; number of stations): Pacific Coast-Northwest (PN, 30), California (CA, 27), Inter-Mountain (IM, 32), Desert Southwest (SW, 24), Central Plains (CP, 62), Texas Hill Country (TX, 22), Midwest (MW, 61), Northeast (NE, 36) and Southeast (SE, 24). The PN and CA regions are composed of stations west of the Pacific Divide. The station locations are shown in Figure 1 and the locational summaries are in Table 1. We use the precipitation year October to September, so for example the Pacific Northwest sample begins October 1 1893 and ends September 30 2025.

Region	Code	Number of stations	Start year
Pacific Northwest	PN	30	1893
California	CA	27	1893
Inter-Mountain West	IM	32	1893
Southwest	SW	24	1893
Central Plains	CP	61	1893
Texas Hill Country	TX	19	1893
Midwest	MW	61	1893
Northeast	NE	36	1888
Southeast	SE	24	1872
Atlantic South	AS	25	1888
Gulf South	GS	38	1888

Table 1: Regions, distribution of stations and start year of data in each region.

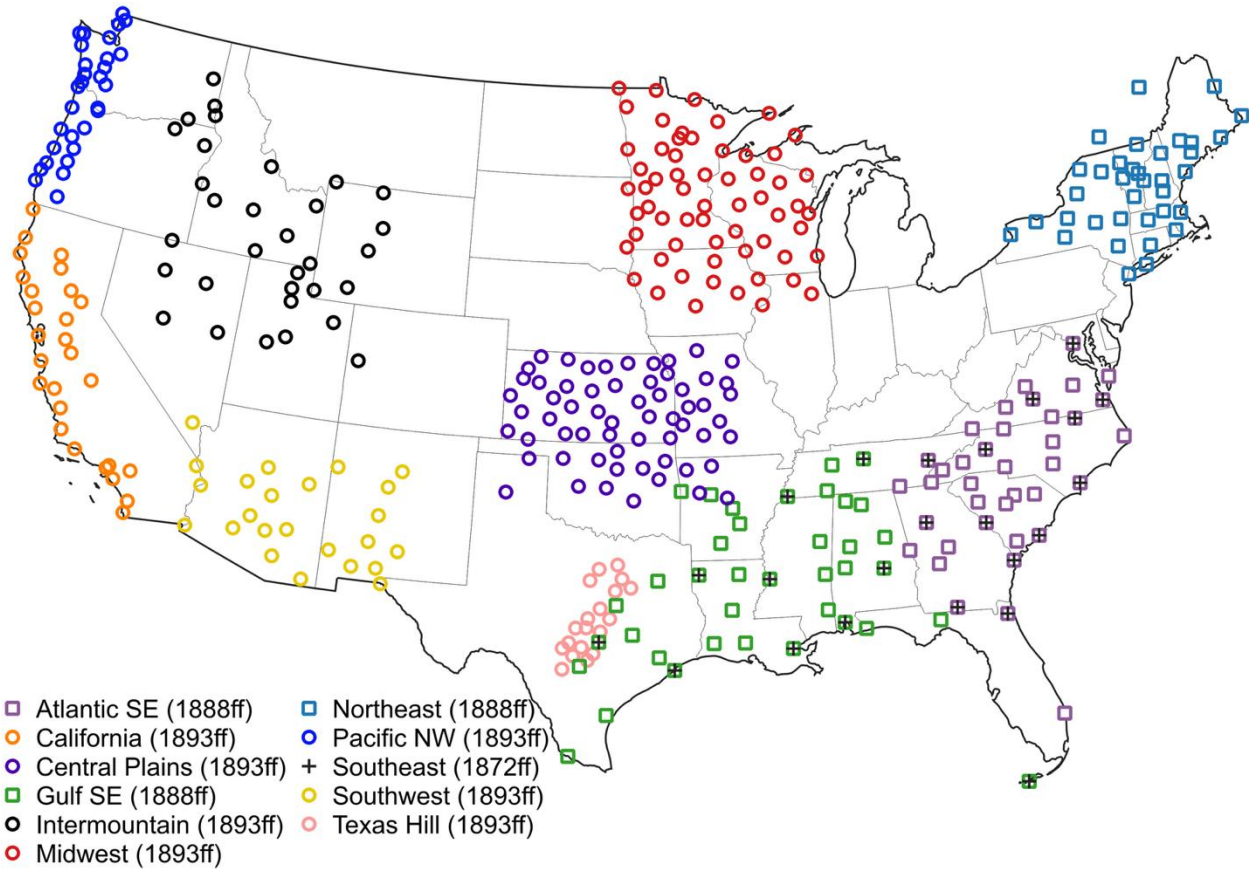


Figure 1. Locations of the 377 stations utilized in this study. All stations in each region are complete for the identified time period. Note a subset of stations in the Gulf South and Atlantic South regions form one combined region, “Southeast”, (+) with observations beginning in 1872.

Archival sources

The source of the daily precipitation values used to construct the time series was the archive maintained by NOAA’s National Center for Environmental Information (NCEI). The basic metric utilized in this study is the 24-hour amount of the liquid-equivalent of precipitation (i.e., including melted snow) measured to 0.01 inch (0.25 mm). Until electronic instrumentation was deployed in the late 20th century, virtually all observers used the standard 8-inch (203 mm) diameter “bucket” gauge topped with a funnel. The funnel drained the precipitation into a tube whose cross-sectional area was one tenth that of the bucket’s, thus magnifying the depth of the precipitation in the tube by a factor of 10 to allow a measurement precision of 0.01 inch.

Beginning in 1991 the National Weather Service replaced manual rain gauges across the country with automated gauges as part of the changeover to the Automated Surface Observing System or ASOS (Butler and McKee 1998, McKee et al. 2000). Equipment changes were subsequently found to change the recorded catch, with some evidence that ASOS sensors undercounted rainfall compared to manual gauges (McKee et al. 2000, NASEM 2012), although use of wind shields raised catch amounts (Dochon and Essenberg 2001). We will include a statistical control for the equipment changeover in our modeling work below.

Prior to 1960 some stations recorded the liquid-equivalent of snow as 10% of the depth of new snow that had fallen rather than melting the snow for a direct measurement. While this introduces error relative to the true melted value, the extreme events of interest here occur during warm season storms (except along the Pacific Coast where near-sea level elevations rarely experience heavy snow) and thus are not affected by this nuance.

The precipitation values were gathered from on-line digital files supplemented with values we manually-keyed from images of the original forms from the NCEI EV2 image archive. An example is shown in Fig. 2 which displays the daily climate information recorded at the Cotton Region Station in Kerrville Texas for July 1900 (a station used in this study). Unfortunately, most of the Cotton-Region Stations, which provided excellent data during the late 19th century, were not keyed into the NCEI archive, and thus are unavailable to researchers who usually rely only on computer-readable files from NCEI.

The example shown here of Kerrville is especially important relative to the 4 July 2025 flooding disaster and the context in which it occurred. Note the rainfall value on 15 July 1900 of 11.60 inch (295mm) and the extensive flooding associated with the event, indicating that the river level rose by the same amount in 1900 as in the 2025 event. However, if querying the NCEI digital archive for the most extreme daily precipitation for Kerrville (NCEI available data for 1901-1974), the value returned is 8.25 inch (210 mm) on 23 June 1965. (A nearby Kerrville station, Kerrville 3 NNE, operating 1974- present, also recorded 11.60 inch (295 mm), on 2 Aug 1978.) The more extreme value from 1900 for the original Kerrville station is not available because the observer did not begin recording the daily data on separate Cooperative Observer forms (which were keyed by NOAA) until 1 Dec 1901. Many stations such as Kerrville were completed for this study back to at least 1893 from such images, providing a more suitable, consistent and complete sample from which analyses may be performed.

U. S. DEPARTMENT OF AGRICULTURE, WEATHER BUREAU.

Monthly Meteorological Record of Cotton-Region Station at *Kerrville, Texas* during *JULY*, 189*0*.

DATE.	TEMPERATURE.*			PRECIPITATION IN INCHES AND HUNDRETHS.			State of weather.	Time observation was taken. A. M.	Time report was filed at telegraph office.	GENERAL SUMMARY.
	Max.	Min.	Moist. <i>Range</i>	Began.	Ended.	Amount.				
1	89	71	18			.00	Clear	6:10	7:00	Mean temperature (obtained by dividing the sum of the mean maximum and mean minimum by two), <u>80.8</u> . Highest temperature during month and date, <u>98</u> . <u>28th & 29th</u> . Lowest temperature during month and date, <u>63</u> . <u>11th & 12th</u> . Total precipitation during month <u>15.59</u> inches. Number of days on which .01 or more precipitation occurred <u>8</u> . Greatest precipitation in any 24 consecutive hours <u>11.60</u> and date, <u>15th</u> . REMARKS. (Note severe storms and unusual phenomena.) <u>Severe rain storm occurred on 15th causing 33ft. rise in river at this station - Highest since has been since 1866 - Much damage to Bridges, land, fences, crops, cotton gins and other plants in path of flood - Flood came suddenly during night - Began rising 9 P.M. - highest 1st AM. - Receding 3 AM - Roads very badly damaged - all telegraph & telephone service delayed several days - No mail for 6 days - No trains 11 days - Damage to Bridges and track on S.A. & A.P. RR estimated \$125,000.00 - Heavy rains on headwaters of Guadalupe during 26th caused 4.5ft rise -</u>
2	90	72	18			.00	"	"	7:00	
3	90	70	20			.00	"	"	6:43	
4	90	70	20			.00	"	"	6:25	
5	87	70	17	5:45 PM	6:45 PM	.10	Partly Cloudy	"	6:47	
6	84	68	16	4:25 PM	7:45 PM	.26	"	"	6:39	
7	88	69	19			.00	Clear	"	6:20	
8	99	78	11			.00	"	"	6:47	
9	90	69	21			.00	"	"	6:47	
10	88	65	23			.00	"	"	6:38	
11	89	63	26			.00	"	"	6:37	
12	92	63	29			.00	"	"	6:25	
13	93	67	26			.00	"	"	6:50	
14	89	71	18	7:45 AM	8:45 AM	1.40	Cloudy	"	6:25	
15	83	73	10	6:45 AM	12:45 AM	11.60	"	"	6:50	
16	89	73	14			.00	Clear	"	6:50	
17	85	72	13	8:45 AM	11:45 AM	.28	Cloudy	"	6:13	
18	86	75	11			.00	Clear	"	6:50	
19	85	75	10			.00	"	"	6:20	
20	89	74	13			.00	"	"	6:50	
21	89	76	13			.00	"	"	6:22	
22	88	76	12			.00	"	"	6:22	
23	90	78	12			.00	"	"	6:20	
24	88	78	10			.00	"	"	6:20	
25	88	76	12			.00	"	"	6:28	
26	90	74	16	11 AM	6:45 AM	1.30	Partly Cloudy	"	7:14	
27	97	74	23	6:10 AM	9:25 AM	.28	Partly Cloudy	"	6:25	
28	98	73	25			.00	Clear	"	7:23	
29	98	74	24			.00	"	6:25	6:18	
30	92	76	16			.00	Partly Cloudy	6:10	6:18	
31	84	72	12	12:20 PM	7:10 PM	.37	Partly Cloudy	6:20	6:40	
Sums	2767	2239	528			15.59				
Means	89.2	72.2	15.0			5.03				

NOTE.—Observations are made as nearly as practicable at 8 a. m., 75th meridian time, or 7 a. m., 90th meridian time.
* For the 24-hour period ending at time of observation; as a rule the maximum being that for the previous day, and the minimum for the current day.

Allen
Observe
[5,000, 1898.]

E. & G. L. Lelaine

J. H. Parsons
"Agent for Observer" Cotton-Region Observer.

Figure 2. Image of the July 1900 Meteorological Record for the Cotton-Region Station at Kerrville, TX. Note the value of 11.60 inches on 15 July, which is the greatest amount in the entire record for the original Kerrville station, yet is not part of the NCEI keyed archive.

In addition to the time-consuming task of manually keying-in non-keyed values, considerable human intervention was required to assess the appropriate designation of “missing” values (typically noted as “M” in the electronic data records). The most tedious issue regarding missing values was contending with the conflicting instructions given to the original keyers regarding precipitation cells on the paper forms that were left blank. Most keyers were instructed to enter zero for a blank cell, but a significant portion were instructed to enter “M”, or “missing” if the cell were blank. The observers themselves would, almost universally, leave the cell blank if no precipitation was measured that day. As a result, several thousand station-months were keyed with one of two entries, (1) the positive amount of precipitation or (2) “M” if the cell were blank, implying that no zero values (the most common entry in reality) ever occurred. This keying error required the examination of approximately 30,000 monthly forms with “missings” to assure the proper values of zero replaced erroneously recorded “M”s.

In other, fortunately many fewer cases, the observer in fact did not measure the precipitation for a month, but submitted the form in any case. Those keyers who replaced all blanks with “zeros” then created an erroneous data listing. While this artifact was found many times in the NCEI snowfall datasets (Christy 2022), it was found less for liquid equivalent. As noted above, since all values of “M” were checked with surrounding stations, substitutions from nearby observers provided values to replace the erroneous “zeros” when such cases occurred.

This did not solve another issue related to erroneous missing values. Some actual values that were recorded on the forms were subsequently changed to “M”. We speculate that the values did not fit a particular quality-control algorithm, so were set to missing in the quality-control processing step. As noted, in our construction of the datasets we examined every entry listed as missing. The example in Figure 3 displays the monthly form for Holdenville Oklahoma for July 1958. In this example, the difference between the on-line accessible values (Table 2) and the actual values is significant. The three days of heaviest precipitation were the 10th, 17th and 21st with 4.55 inch (116 mm), 2.87 inch (73 mm) and 2.95 inch (75 mm) respectively. However, in the NCEI-accessible archive, these values are listed as missing even though the values were clearly written on the form and other nearby stations reported heavy rain as well. Once again, by examining every value that was listed as missing in the digital archives, we are able to provide more accurate information, especially regarding extremes, by checking the original forms.

1950-07-04	0.22
1950-07-05	0.59
1950-07-06	0.00
1950-07-07	0.00
1950-07-08	0.00
1950-07-09	0.22
1950-07-10	M
1950-07-11	0.00
1950-07-12	0.00
1950-07-13	0.04
1950-07-14	0.05
1950-07-15	0.00
1950-07-16	0.00
1950-07-17	M
1950-07-18	0.00
1950-07-19	0.00
1950-07-20	1.10
1950-07-21	M
1950-07-22	1.30
1950-07-23	0.00
1950-07-24	0.00
1950-07-25	1.39
1950-07-26	0.00
1950-07-27	0.00
1950-07-28	0.11
1950-07-29	1.02
1950-07-30	0.18
1950-07-31	0.09

Table 2. Daily data listing of precipitation (inches) at Holdenville Oklahoma (COOP ID 344235) for July 1950 downloaded 18 Nov 2025 from GHCND archive <https://www.ncdc.noaa.gov/cdo-web/search>.

Stations

By 1893, the U.S. Weather Bureau was at an organizational stage such that regular, standardized monthly forms of daily data were being generated and archived for stations across the CONUS. This then became the default start-date for the stations utilized in this dataset. However, the U.S. Signal Corps and other organizations had been recording weather observations prior to this time. Three regions provided enough information to begin all station records in 1888 (NE, GS and AS). Further, there were enough stations (24) in the GS and AS regions for continuous data to be constructed since 1872, which were combined and denoted as Southeast (SE). The tight clustering of stations in central Texas (see Figure 1) was generated to create a sample that was capable of representing the relatively smaller region known as “Flash Flood Alley”.

2.2 PRELIMINARY DATA EXPLORATION

2-day precipitation extremes

To give the reader an introduction to the overall characteristics of extreme events and the types of analyses to follow we present in Fig. 4 information about 2-day precipitation totals (a metric examined below). In this figure, we have calculated the heaviest 2-day precipitation total for each station in each year, then normalized each station's yearly value by the mean of that metric over all years for that station. A value of 1.0 for a given year implies that the heaviest 2-day rainfall total for that year matched that for the mean for all years. This normalization is important as there can be a wide range of absolute mean values among all the stations in a given region. We then averaged these values up within each region and took the running 7-year centered average.

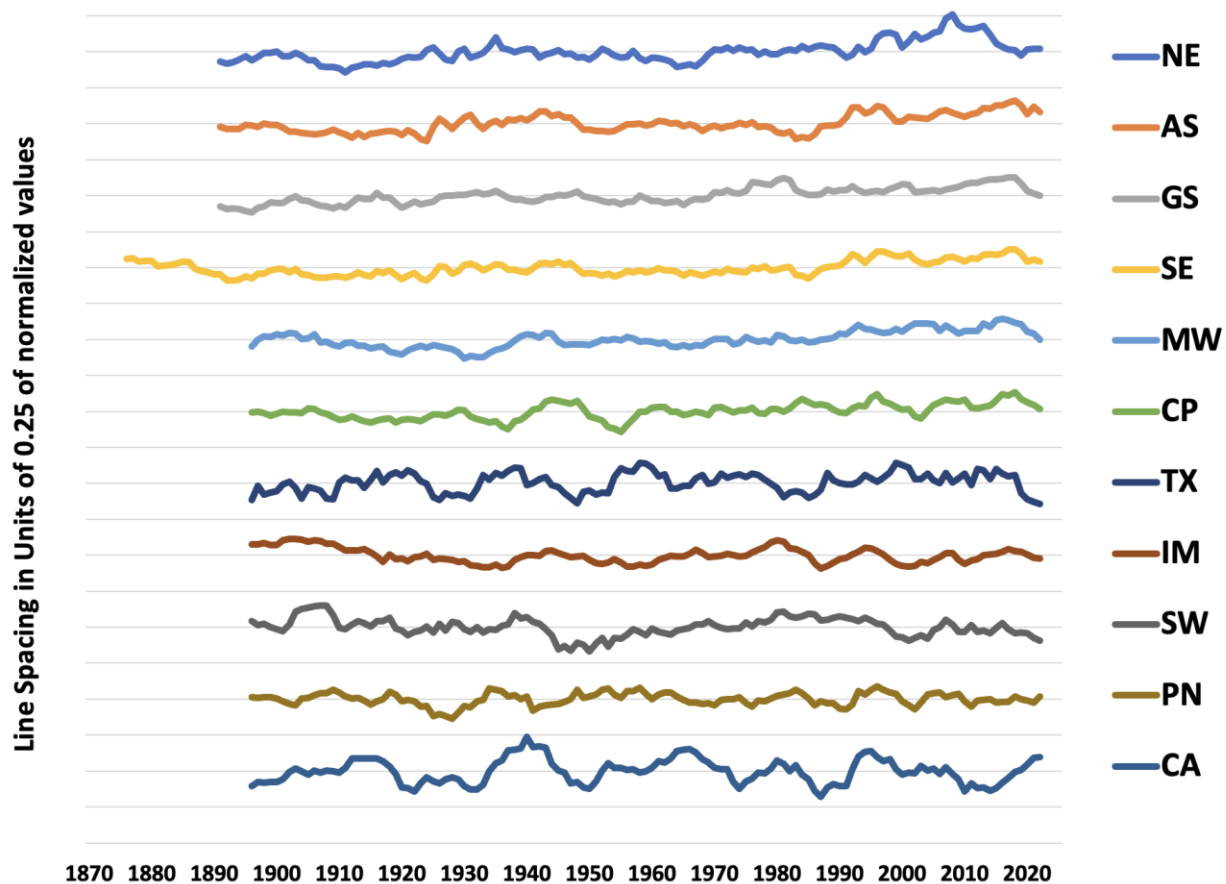


Figure 4. Time series of regional averages of normalized amount of precipitation falling on the heaviest 2-day event each year. The time series is a 7-year running, centered average.

Figure 4 displays the results. The most interesting feature is the peak of values (1.26) in the NE during 2005-2011 which corresponds to the peak of increased tropical storm activity that occurred from 1995 to 2014 in the region (Jong *et al.* 2024). The SE, AS, GS and MW exhibit an upward shift around 1990, representing a magnitude change of about 7%, followed by a leveling. As noted above, part of this increase may be due to the installation of wind-shielded gauges. The five western

regions (TX, IM, SW, CA and PN) are characterized by variations, due partly to a smaller sample of stations, but no unusual long-term behavior.

Northeast 99th percentile

In Figure 5 we show a second example of the type of analysis we employ. Here is displayed the time series of the NE regional total amount of precipitation falling during the heaviest 1 percent of 1-day events.¹ The data are normalized so 1958 = 1.0. The postwar period had the fewest events since 1888 and there was a concentration of aforementioned heavier events in 1995-2014. The graph qualitatively confirms the increase reported in NCA5, but inspection also shows that postwar trend is not monotonic upward. This demonstrates the need to consider periods of different lengths to understand—and better-represent—trends and their potential causes.

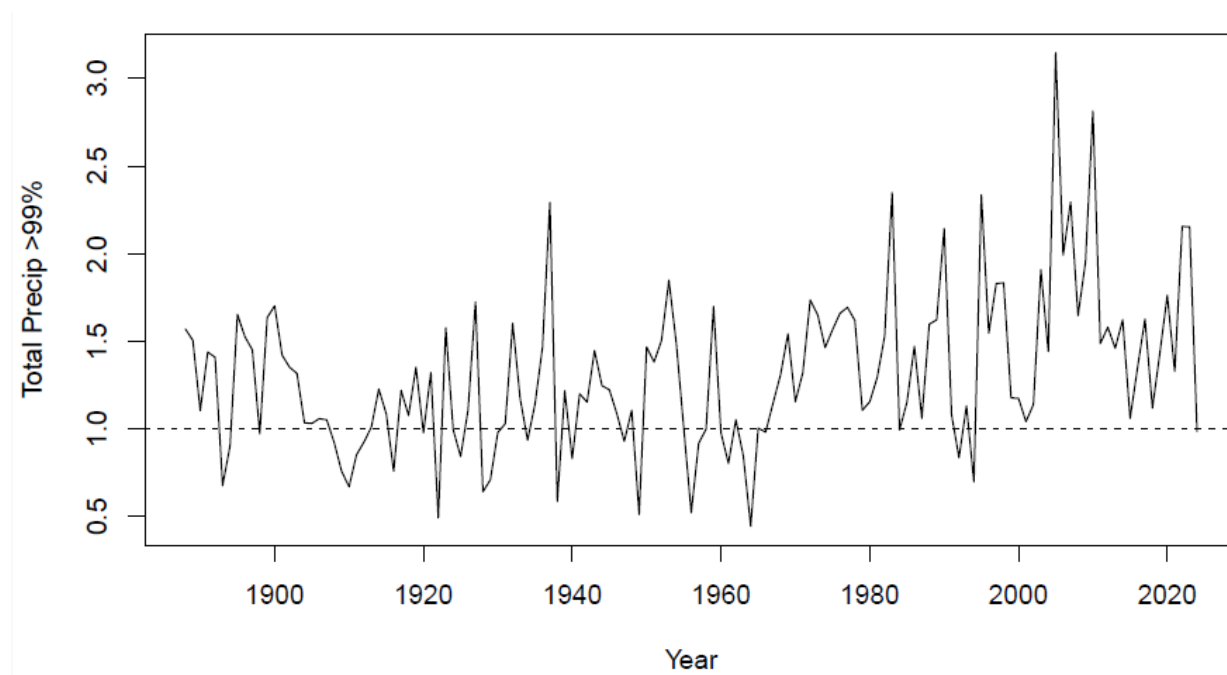


Figure 5. Time series of the annual total of precipitation in the Northeast region which occurred on those days in which the total exceeded the 99th percentile of all precipitating days. The value is the total across 36 stations, 1888 to 2024, normalized so 1958 = 1.0.

We now turn to the metrics that will be derived from the 377-station dataset.

2.3 PRECIPITATION METRICS

The data are grouped into precipitation years (October to September). February 29 values for leap years are removed so each year has 365 days. The metrics fall into three groups: precipitation totals, clustering indicators and extremes. The totals are represented by annual sums of 1-day and 2-day rainfall totals. Clustering measures are the annual average on non-zero days, annual skewness and the summertime (June to September) totals. Extremes are measured as the annual maximum 1-day value and the total precipitation falling on days comprising the heaviest 1 percent

¹ Specifically, days were selected on which total precipitation was in the 99th percentile of all days in the sample and the metric consist of the annual sums of the selected days, divided by the 1958 value.

of all precipitation events in the sample at that location (so-called 100 year events). We refer to the latter as 99th percentile exceedances. Following Jorgensen and Nielsen-Gammon we use the log of the annual block maximum although this step is not influential on the results. We expect the 1-day and 2-day totals to behave similarly and the results show that to be the case. A difference in results between annual totals and the average on non-zero days would indicate if rainfall is becoming more or less concentrated during the year. An increase in skewness indicates if more and more extreme upper-tail events are occurring, and vice-versa.

Metric name	Short form	Definition
1-day total	Total	Sum of 365 daily rainfall totals
2-day total	2-day_Tot	Sum of 365 pairs (today+yesterday) totals
Average on nonzero days	NZ_average	(Total rain on days with non-zero rain) / (number of days with non-zero precipitation)
Skewness	Skewness	Asymmetry of distribution (positive value implies right-skewed)
Log(Maximum)	Maximum	Log of the highest annual value
99 th percentile exceedances	99 th _Exceed	Total precipitation on days per year for which precipitation is in top 1% of observations at that location
Summertime total	Summer-Tot	Total June-September precipitation

Table 3: Metric names, codes and definitions.

Note that the metrics in Table 3 are applied to records at individual locations. The regional aggregates are formed by averaging the location-specific metrics. So, for instance, the regional “maximum” is the average of the location-specific log-annual maxima across the region that year. As such it may combine data on rainfall events on different days. An alternative approach would be to take the maximum of location-specific maxima across a region. None of the conclusions derived below would change if we used this approach instead.

3 ANALYSIS

3.1 TREND ANALYSIS

We estimate linear trends in all individual locations and regional averages over three time scales: the entire sample (1893 or earlier to 2025), 1958—2025 and 1980—2025. Each subsample is of sufficient length that if trends in annual metrics are present, we will detect them. The linear trend model is

$$y_{i,t} = \alpha_i + \beta_i t + e_{i,t}$$

where y is the precipitation metric, i denotes the location, t denotes the year, and $e_{i,t}$ denotes the regression residual. We obtain standard errors by modeling persistence in the error terms using the non-parametric covariance matrix of Vogelsang and Franses (2007). This is like a serial correlation adjustment but is adapted to each data set to accommodate autocorrelation lags of unknown length. The Vogelsang and Franses (2007) estimator is in the tradition of Heteroskedasticity and Autocorrelation Consistent (HAC) covariance matrix estimators common in econometrics and has some similarities to the well-known Newey and West (1987) estimator. The

Vogelsang and Franses (2007) estimator takes advantage of properties of the deterministic trend model to reduce size distortions, i.e. reducing the tendency to over-reject a true null, without losing power to reject a false null.

Altogether we conduct 8,148 trend tests (7 metrics on 3 time samples at 377 individual locations plus 11 regional averages). All individual trend results (trend coefficient and 95% confidence intervals) are available in the Supplementary Information annex.

Figures 6 and 7 present top-level summaries of results, each one showing for each region and interval the percent of stations in the region exhibiting, respectively, a positive or negative trend. The top-left box in Figure 6 shows that in the Pacific Northwest Coast (PN) region over the entire post-1893 sample a significant positive trend was detected in annual total rainfall in three percent of stations (1 out of 30). The next two boxes down the column show that this falls to zero for the later PN subsamples. For CA a positive trend is detected after 1893 in 4 percent of stations (1 out of 27) and zero on the later subsamples. Figure 7 shows that significant negative trends were detected in the PN region annual total precipitation in three percent of locations after 1893 and 1958, rising to seven percent (2 out of 30) after 1980.

The regions are listed in approximately west-to-east order, so the gradient in annual total rainfall previously noted (Kunkel et al. 2020) is visible. Positive trends outnumber negative ones in the east, and vice-versa in the west. The Northeast (NE) region yields the greatest fraction of positive trends in daily totals with 47, 61 and 31 percent reporting upward trends on samples beginning, respectively, in 1888, 1958 and 1980. 39 percent of stations in the NE exhibit an increasing trend in 99th percentile exceedances on the sample beginning in 1958, lending support to the statement in NCA5 discussed above. But that appears to be driven as much by the low postwar levels as the high post-1980 levels since on the subsample beginning in 1980 the fraction falls to only 3 percent, opposite to what we would expect if the trend were driven by global climate change. Likewise, while 50 percent of NE stations exhibit an upward trend in summertime precipitation after 1958 the fraction falls to 11 percent after 1980, and while 22 percent exhibit an upward trend in the annual maximum after 1958 none do after 1980.

The Gulf South is another region exhibiting a strong regional trend in daily totals, although only when measured on the longest time scale (post-1888). After 1958 the incidence of trends drops considerably. The opposite is observed in the Atlantic South where the incidence of trends rises in later subsamples. Also, 40 percent of stations there exhibit a positive trend in 99th percentile exceedances after 1980, although only 20 percent of locations have a trend in the annual maximum, demonstrating that even related metrics can yield contrasting results.

Summertime total rainfall exhibited a significant negative trend in 63 percent of PN stations (19 out of 30) after 1980, though this is the driest part of the year so trends can reflect small changes in absolute terms. Negative trends in non-zero day totals became less common after 1958. In the IM region summertime rainfall declined in 31 percent of stations after 1958. There were negative trends in 1- and 2-day totals in half the SW stations on the post-1980 sample. Otherwise, significant negative trends were observed in fewer than half of regional stations in all metrics on all time scales, indeed in most cases fewer than ten percent.

Skewness shows some tendency to increase in the PN and CA regions on later subsamples, although in those areas there is no trend in the non-zero day-average. No other region exhibits noteworthy increasing or decreasing skewness. There is little tendency for higher annual maxima over the full sample lengths and no emergence of stronger patterns on the post-1980 subsample. In TX there are

more stations exhibiting significant declines in annual maxima after 1958 than increases, although the percentages remain small. Finally, the summertime total shows little tendency to trend up except, as noted, in the NE post-1958 (but not post-1980) and down in the PN region post-1980.

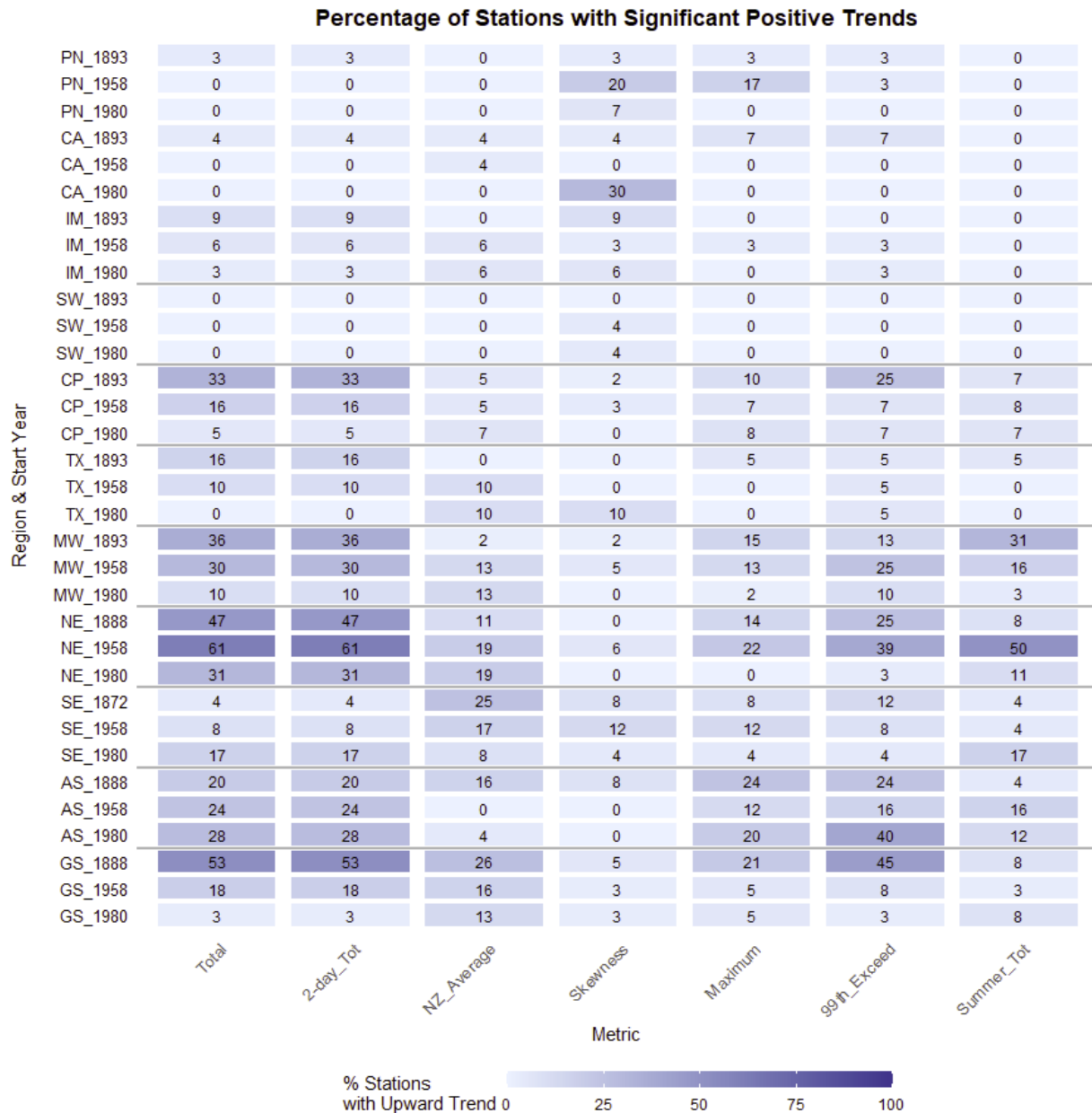


Figure 6: Trend detection in U.S. precipitation data. Each row is a region with the sample start year as indicated (end year is always 2024). Columns are precipitation metrics as indicated. The number shown is the percent of stations in that region in which a positive and statistically significant trend (at 5%) in that metric was detected on that time scale. Color-coding is added as an aid to visualization.

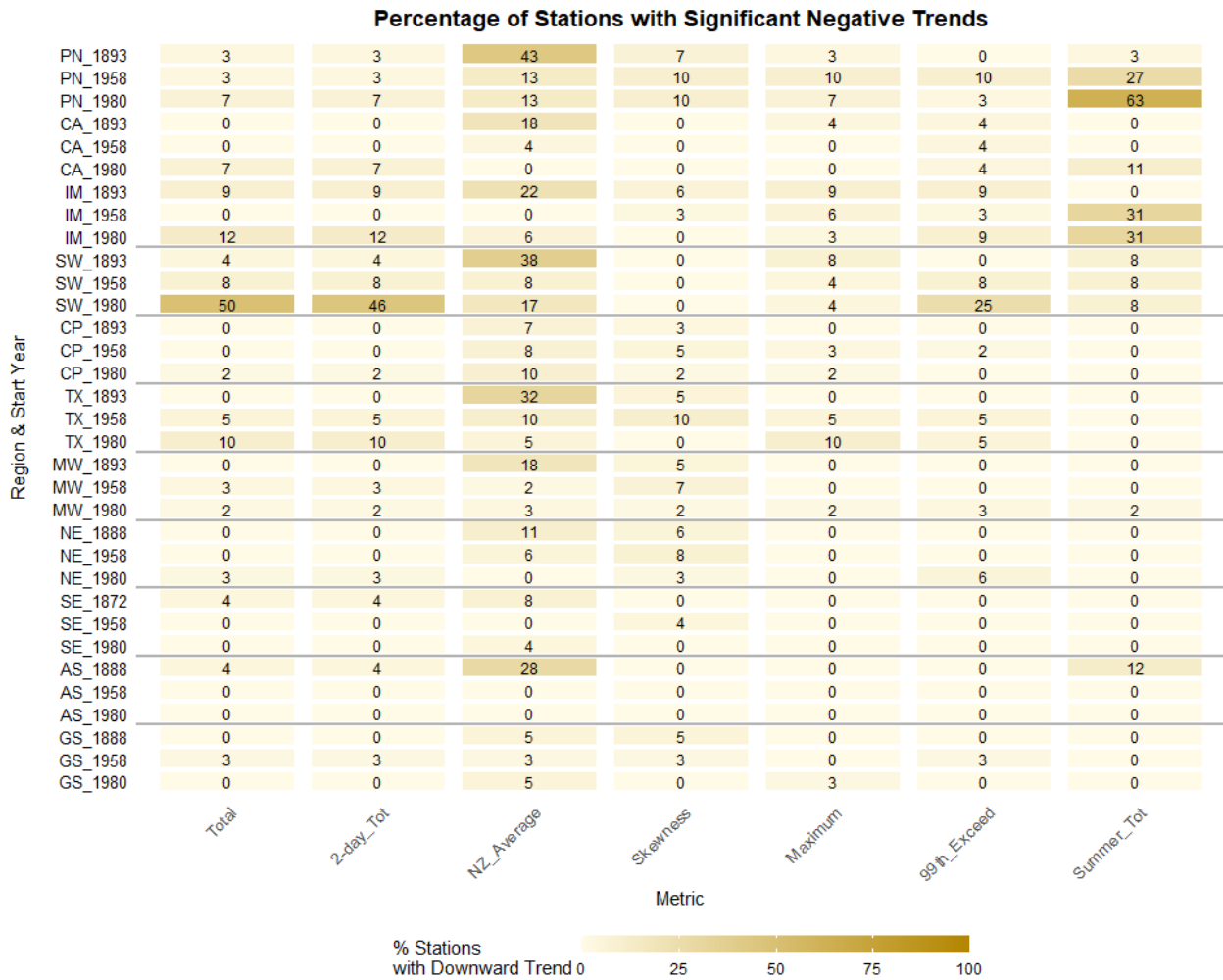


Figure 7: As for Figure 6 but detection of negative and statistically significant (at 5%) trends.

Regional average results

Results for the regional averages are shown in Table 4. If no significant trend was detected the cell is blank, -1 indicates a negative trend was detected and +1 indicates a positive trend was detected. All regions exhibit at least one trend in one metric. The western regions are more likely to exhibit negative trends than positive ones, and vice-versa for the east. If we define robust trend detection as a directional finding on the post-1958 interval that is sustained on the post-1980 time scale, we detect one such change in the IM region (declining summertime total rainfall) and in the Southeast (increasing maximum rainfall). No other region exhibits such a finding for any metric. The NE, CP and MW regions exhibit upward trends in annual totals and extremes on earlier samples but not on the post-1980 subsample. The PN region shows a negative trend in the summertime total post-1980 but not before, while the non-zero day-average trends down prior to 1980 but not after. TX exhibits a decline in rainfall on non-zero days post-1893 but not after 1958 or 1980. Likewise, the SW is unremarkable on long time scales but exhibits indications of declining total and extreme rainfall after 1980.

	Start year	Average	2-day Tot	NZ Average	Skewness	Maximum	99th Exceed	Summer Tot
PN	1893			-1				
PN	1958			-1				
PN	1980							-1
CA	1893			-1				
CA	1958							
CA	1980				+1			
IM	1893							
IM	1958							-1
IM	1980							-1
SW	1893			-1				
SW	1958							
SW	1980	-1	-1				-1	
CP	1893	+1	+1			+1	+1	
CP	1958						+1	
CP	1980							
TX	1893			-1				
TX	1958							
TX	1980							
MW	1893	+1	+1			+1		+1
MW	1958	+1	+1			+1	+1	
MW	1980							
NE	1888	+1	+1					
NE	1958	+1	+1				+1	+1
NE	1980							
SE	1872							
SE	1958			+1		+1	+1	
SE	1980					+1		+1
AS	1888					+1		
AS	1958							
AS	1980					+1	+1	
GS	1888	+1	+1			+1	+1	
GS	1958						+1	
GS	1980							

Table 4: Summary of trend detection in regional averages by metric and time sample. -1 = significant (at 5%) negative trend; Blank = no trend; +1 = significant (at 5%) positive trend.

In sum, other than for summertime rainfall in the Inter-Mountain region and maximum rainfall in the Southeast we do not robustly detect any post-1958 national or even region-wide patterns in measures of total, clustered or extreme precipitation. While individual locations exhibit such trends on some time scales there are very few cases in which the majority of stations in a region, and the region-wide average, follows the pattern.

3.2 GEV ANALYSIS

The 5th National Climate Assessment asserted that the frequency and intensity of heavy precipitation events scales with the global warming level (e.g. Marvel et al. 2023 p. 2-24). In this section we examine the behavior of annual maximum precipitation by fitting a nonstationary Generalized Extreme Value (GEV) distribution (Reiss and Thomas 2007) at each location using the log of the annual maximum precipitation, allowing the location parameter to vary linearly with the global mean surface temperature anomaly ($GMST_t$), for which we use the annual HadCRUT value obtained from <https://climate.metoffice.cloud/temperature.html#datasets> on November 3, 2025. It is customary to interpret a significant coefficient on $GMST_t$ as “attribution” to climate change or greenhouse gases, although there are many caveats to equating partial correlation with causation. There is a significant danger of omitted variables bias if relevant causal variables are left out of the model (see, e.g., Sherman et al. 2025) so we add two additional covariates. The first is the El Niño-Southern Oscillation index obtained from <https://psl.noaa.gov> (downloaded January 8 2026). The second is a dummy variable taking the value 0 up to 1990 and 1 thereafter, to control for potential artifactual changes in measured precipitation at the time of the change from manual to ASOS gauges. Jorgensen and Nielsen-Gammon (2024) discuss other choices of explanatory variables. The log of the atmospheric CO₂ concentration can be used as a measure of anthropogenic forcing, although as they note it leaves out regionally-important effects of aerosols. Also the log CO₂ time series has a unit root (Hartley 2025) which means its use in a linear regression model without confirming cointegration with the other variables in the model yields biased and invalid standard errors (Davidson and MacKinnon 2004). Jorgensen and Nielsen-Gammon (2024) propose the ensemble average $GMST_t$ from climate models as a proxy that removes the influence of ENSO-type signals, but here we simply include ENSO directly as a control.

Since we are analyzing data from all regions using all available time periods we are not applying an event-contingent stopping rule, thus we avoid the potential bias that affects extreme event attribution when the location and sample length are chosen based on observation of an exceptional weather event (Miralles and Davison 2023). As is customary in GEV modeling we assume all observations are independent and no correction for serial correlation is applied.

Altogether we fit 1,164 GEV models (377 locations plus eleven regional averages and three time periods). The fit is optimized using Maximum Likelihood as implemented in the extRemes package in R (R Core Team 2023). While use of the nonparametric bootstrap is common in GEV applications, it can yield confidence intervals that are too narrow especially in modest sample sizes (Kysely 2008). We test the exclusion of the $GMST_t$ coefficient two ways. One, following the approach of Sherman et al., we computed a likelihood ratio statistic (also called a deviance statistic) comparing the optimized likelihood value of the unrestricted model and an alternative model restricted so the location parameter does not depend on $GMST_t$, the value of which is distributed $\chi^2(1)$ under the null (Davidson and MacKinnon 2004). We also used the empirical Hessian matrix to generate

coefficient variances which are then used to construct 95% confidence intervals, and we checked whether they encompass zero. This method assumes local symmetry of the coefficient distribution. Both methods yielded the same inferences.

Table 4 summarizes the results (all station-specific results are available in the Supplement). The dependent variable is the regional average of station-specific annual maximum precipitation. A 0 indicates a null result, 1 denotes a significant positive coefficient on $GMST_t$ on a sample with a significant trend, and (1) indicates the $GMST_t$ coefficient is significant but not the trend term. In the Northeast, Atlantic South and Gulf South regions we find a significant positive coefficient on $GMST_t$ on the longest time scale but it is not significant in those regions on the later subsamples. The coefficient magnitudes (not shown but available in the supplement) can be interpreted as the percentage change in maximum annual rainfall per °C of global warming. They also drop in size. For the AS region they are 0.27 (i.e. +27% per °C) in the post-1888 sample, 0.17 post-1958 and 0.16 post-1980. In the GS region case the coefficients are, respectively, 0.41, 0.30 and 0.36 and in the NE they are 0.100, 0.106 and 0.052 respectively. In no other case do we achieve attribution.

	PN	CA	IM	SW	CP	TX	MW	NE	SE	AS	GS
Earliest	0	0	0	0	0	0	0	(1)	0	1	1
1958	0	0	0	0	0	0	0	0	0	0	0
1980	0	0	0	0	0	0	0	0	0	0	0

Table 4: Summary of GEV analysis on annual maximum precipitation. 0: no significant effect. (1): significant coefficient on $GMST_t$ but no significant trend. 1: significant $GMST_t$ coefficient and significant trend.

Since temperature and ENSO are global, the failure to achieve attribution across regions requires further explanation. Many of the $GMST_t$ location parameters summarized in Table 4 are positive but not statistically distinguishable from zero in the context of observed natural variability. Inclusion of the 1991 dummy variable is influential on the Table 4 results. If it is omitted the results are as shown in Table 5. Attribution now happens in the SE and AS post-1950, the MW prior to 1980 and in the IM and CP on the longest samples. The prior attribution in the GS region on the longest sample disappears. The sensitivity of the results to presence of the dummy variable argues for its inclusion since it is known *a priori* that there were influential nationwide changes in measurement equipment after 1991. Additionally, Bishop et al. (2019) noted that increased precipitation in the SE over 1895—2016 was primarily in the fall and was driven by increased moisture transport from the Gulf of Mexico and Caribbean which they attributed to enhanced winds over the North Atlantic, not to anthropogenic forcing, again indicating that the attribution results in Table 5 are potentially spurious due to omitted variables bias.

	PN	CA	IM	SW	CP	TX	MW	NE	SE	AS	GS
Earliest	0	0	(1)	0	1	0	1	(1)	0	1	0
1958	0	0	0	0	0	0	1	(1)	1	(1)	0
1980	0	0	0	0	0	0	0	0	1	1	0

Table 5: As for Table 4 but omitting the post-1991 dummy variable in the GEV model.

3.3 PANEL REGRESSION ANALYSIS

While it has become common to rely on GEV models to examine the behavior of weather extremes, other methods offer some distinct advantages, and all have inherent limitations. Inferences for linear regression analysis when the dependent variable is not Gaussian rely on asymptotic analysis of the error terms, but the GEV distribution itself is an asymptotic approximation based on strong assumptions about independence of the observations (Reiss and Thomas 2007), so it is not automatically more valid. Conventional regression models have the advantage of offering a larger suite of well-understood methodological tools for reducing bias, including specification tests and methods for computing consistent standard errors.

Here we exploit the sample size created when the region-wide records are pooled, that is, stacked end to end. We focus specifically on the shortest time interval (starting in 1980) to address whether the failure to find attribution on subsamples is due to a deficient sample size. Using that interval also allows us to use lower troposphere satellite temperature retrievals as explanatory variables. Panel regression involves using repeated time series measures across locations which boosts the sample length, but obtaining consistent standard errors requires correcting for spatial and temporal dependence, which we do using the covariance matrix estimator of Driscoll and Kraay (1998). The simplest panel regression model allows for each region to have a separate intercept but common slope coefficients. Here we allow western regions (PN, CA, IM, SW and MW) to have different slopes on the temperature measure as well, reflecting potential heterogeneity in the regional response to global warming. The regression model is

$$\log(y_{i,t}^x) = \alpha_i + \beta_1 Temp_t + \beta_2 DW_i \times Temp_t + \beta_3 ENSO_t + \beta_4 D91_t + e_{i,t}$$

where $y_{i,t}^x$ is the regional average of the annual maximum 1-day rainfall events, α_i is a vector of intercepts allowing a unique value for each region, $Temp_t$ refers to the temperature measure which varies by year but is common across regions, DW_i is a dummy variable taking the value 1 if the region is in the west and 0 if in the east, $ENSO_t$ is the El Niño Index, $D91_t$ is a dummy variable taking the value 0 up to 1990 and 1 thereafter, the β 's are slope coefficients to be estimated and $e_{i,t}$ is the regression error term. Since the dependent variable is in logs the regression coefficients can be interpreted as percent changes in regional maximum precipitation for a one-unit change in the explanatory variable. The effect of temperature on log-max precipitation in the eastern regions ($DW_i = 0$) is measured by $\hat{\beta}_1$, and the effect for western regions is measured by $\hat{\beta}_1 + \hat{\beta}_2$. We measure temperature using 3 data products: HadCRUT global mean surface temperature as before, and the global and CONUS-wide Lower Troposphere (LT) Microwave Sounding Unit-measured temperature series version 6.1 from the University of Alabama in Huntsville (Spencer and Christy 1992), denoted respectively LT-Global and LT-USA.

The results are reported in Table 5 (the intercepts are not reported). For each temperature product we report the estimates $\hat{\beta}_1$ and $\hat{\beta}_1 + \hat{\beta}_2$, in other words the temperature effects on eastern and western max precipitation respectively. Beneath each coefficient is the p -value on a t -statistic formed using Driscoll-Kraay standard errors, testing that the true value of the reported coefficient is zero. If the p -value is below 0.1 (marginal significance) the coefficient is shown in bold face. The final row reports the sample size. In only one case, when using the UAH LT USA temperature series and only in the east, is there a significant positive effect on maximum regional precipitation. The coefficients are of similar size (approximately 0.06—0.09) implying 6—9 percent increases in maximum precipitation per 1°C LT warming. The difficulty of invoking a physical principle like Clausius-Clapeyron to explain this is that the effect disappears in the western part of the continent, even though the laws of physics presumably do not.

	GMST	LT-Global	LT-USA
Temp-East	0.060	0.091	0.062
pr(Temp-East)	0.254	0.070	0.012
Temp-West	-0.020	-0.014	-0.036
pr(Temp-West)	0.584	0.678	0.198
ENSO	0.023	0.021	0.024
pr(ENSO)	0.019	0.045	0.010
D91	0.014	0.010	0.018
pr(91)	0.575	0.632	0.323
<i>N</i>	495	495	495

Table 5. Results of panel regression using three temperature data products.

ENSO also affects precipitation. The index is constructed so that an intense El Niño event take the value +1, so we can say that a strong El Niño adds about two percent to maximum precipitation. The dummy variable for instrumentation change adds between one and two percent but the effect is insignificant. If $D91_t$ is removed from the regression the only changed inference is that the Temp-East coefficient using GMST rises to 0.073 and becomes marginally significant ($p = 0.077$). That on Temp-West shrinks to -0.007 and remains insignificant ($p = 0.800$). The ENSO coefficients remain about the same size and retain their significance.

It is noteworthy that the LT-USA is correlated with GMST ($\rho = 0.743$) and with LT-Global ($\rho = 0.758$) yet its explanatory power for max precipitation is so much stronger. If the explanation is that warming increases potential downpour amounts then it is strange the effect only applies in the east. In the west it is not merely the case that the effect is noisier, the coefficient collapses to zero. An alternative explanation may be that both LT-USA and maximum precipitation in the east are jointly driven by other causal factors not included herein, such as oceanic drivers of Atlantic tropical storm activity, echoing the findings in van der Wiel et al (2016). This would also rationalize the results in the previous section, in which a connection between global average temperature and precipitation extremes is only found in the easternmost regions: we cannot rule out that we have omitted an explanatory factor connected to oceanic changes that affect both temperatures and rates of coastal storm formation. We can, however, rule out identification of a significant, direct causal connection between warming and maximum rainfall, since if that were the case it would not vanish in the west.

4 DISCUSSION AND CONCLUSIONS

Our first aim herein is to publish one of the largest collections of U.S. precipitation records ever assembled, providing complete high quality daily records for 377 locations in nine regions back at least to 1893 and in some areas back as far as 1872. Notwithstanding what can be learned about out-of-sample event probabilities from statistical modeling of recent weather records, the laborious

task of building and examining the longest possible precipitation histories at locations across the country remains, in our view, critical for understanding current and future risks associated with extreme precipitation.

We have also undertaken a comprehensive analysis of trends and potential drivers of observed changes. Over the past 130 years we find, similar to Kunkel et al. (2019), there has been a tendency for increased rainfall in the east and decreased rainfall in the west, although the gradient weakens after 1980 and there is considerable heterogeneity by location and temporal subsample. We find no truly CONUS-wide trends nor attributable changes in any of our measures of average or extreme precipitation. Regional trends observed on the entire post-1958 interval as used in the NCA5 do not typically hold up on the post-1980 subsample or when the sample is extended back to the late 1800s. The Northeast region shows evidence of higher annual total and extreme precipitation after 1958 but the fraction of locations with significant trends drops sharply after 1980 and the regional trends become insignificant on the post-1980 subsample. The Southeast exhibits a robust upward trend in maximum rainfall after 1958 and it, the Northeast and the Gulf South support an attribution of maximum rainfall trends to global warming when analyzed on the longest record, but not on the post-1958 subsample when the warming signal should be strongest. Based on the panel regression results, in which significant effects of temperature on maximum rainfall after 1980 appear in the east but not in the west, we conjecture that what appears to be a causal link with warming may be an artifact of omitting a climatic driver that jointly affects US Atlantic coastal storms and tropospheric temperatures.

Our findings obviously do not mean there is no such thing as extreme rainfall in the U.S. record, or that it does not sometimes exhibit multi-decadal trends up or down in some regions. We have shown these things to be demonstrably true. But our findings do not support the general claim in the Fifth National Climate Assessment (p. 2-24) that the frequency and severity of extreme rainfall scales linearly with the global warming level. There is too much heterogeneity in the record to support such a conclusion. Trends in extreme rainfall can be found in many locations. For the purpose of disaster planning or other applications we encourage users of climate data to study the longest possible time series of local rainfall records. With regards to forecasting extremes we find ENSO informative and regional temperature projections informative in some locations, but projections of global mean surface temperature are unlikely to improve local precipitation forecasts.

References

- Bishop, Daniel A., A. Park Williams, Richard Seager, Arlene M. Fiore, Benjamin I. Cook, Justin S. Mankin, Deepti Singh, Jason E. Smerdon, and Mukund P. Rao (2019) Investigating the Causes of Increased Twentieth-Century Fall Precipitation over the Southeastern United States. *Journal of Climate* Volume 32, <https://doi.org/10.1175/JCLI-D-18-0244.1>
- Butler, R. D. and T. B. McKee. 1998. ASOS Heated Tipping Bucket Performance Assessment and Impact on Precipitation Climate Continuity. Atmospheric Science Paper No. 655, Climatology Report 98-2. Fort Collins, CO: Colorado State University. 83 pp.
- Christy, J.R., 2022: Time series construction of Oregon and Washington snowfall since 1890 and an update on California snowfall through 2020. *Journal of Hydrometeorology*, 23, 1845-1860. Doi:10.1175/JHM-D-21-0178.1.
- Driscoll, John C. and Aart C. Kraay (1998) "Consistent Covariance Matrix Estimation with Spatially Dependent Panel Data" *The Review of Economics and Statistics*, Nov., 1998, Vol. 80, No. 4 (Nov., 1998), pp. 549-560 <https://www.jstor.org/stable/2646837>

- Duchon, Claude E. and Gavin R. Essenberg (2001) Comparative rainfall observations from pit and aboveground rain gauges with and without wind shields. *Water Resources Research* 37(12) 3253-3263. <https://agupubs.onlinelibrary.wiley.com/doi/abs/10.1029/2001WR000541>
- Jong, B.-T., Murakami, H., Delworth, T.L., & Cooke, W. F. (2024). Contributions of tropical cyclones and atmospheric rivers to extreme precipitation trends over the Northeast US. *Earth's Future*, 12, e2023EF004370. <https://doi.org/10.1029/2023EF004370>.
- Kysely, J. (2008). A cautionary note on the use of nonparametric bootstrap for estimating uncertainties in extreme-value models. *Journal of Applied Meteorology and Climatology*, 47(12), 3236–3251.
- Marvel, K., W. Su, R. Delgado, S. Aarons, A. Chatterjee, M.E. Garcia, Z. Hausfather, K. Hayhoe, D.A. Hence, E.B. Jewett, A. Robel, D. Singh, A. Tripathi, and R.S. Vose (2023): Ch. 2. Climate trends. In: Fifth National Climate Assessment. Crimmins, A.R., C.W. Avery, D.R. Easterling, K.E. Kunkel, B.C. Stewart, and T.K. Maycock, Eds. U.S. Global Change Research Program, Washington, DC, USA. <https://doi.org/10.7930/NCA5.2023.CH2>
- McKee, T. B., N. J. Doesken, C. A. Davey, and R. A. Pielke Sr. (2000) Climate Data Continuity with ASOS. Report for Period April 1996-June 2000. Fort Collins, CO: Colorado State University.
- National Academies of Sciences, Engineering, and Medicine (2012) The National Weather Service Modernization and Associated Restructuring: A Retrospective Assessment. Washington, DC: The National Academies Press. <https://doi.org/10.17226/6941>.
- McKittrick, R. and J.R. Christy, 2019: Assessing changes in US regional precipitation on multiple time scales. *Journal of Hydrology* 578, <https://doi.org/10.1016/j.jhydrol.2019.124074>
- Miralles, Ophélie and Anthony Davison (2023) Timing and spatial selection bias in rapid extreme event attribution. *Weather and Climate Extremes* 41 100584 <https://doi.org/10.1016/j.wace.2023.100584>
- Newey, W.K. and K.D. West (1987). A simple, positive semi-definite, heteroskedasticity and autocorrelation consistent covariance matrix. *Econometrica* 55, 703–708.
- R Core Team (2023). R: A language and environment for statistical computing. R Foundation for Statistical Computing, Vienna, Austria. <https://www.R-project.org/>
- Reiss, Rolf-Dieter and Michael Thomas (2007) *Statistical Analysis of Extreme Values with Applications to Insurance, Finance, Hydrology and Other Fields*. 3rd ed. Basel: Birkhäuser.
- Sherman, P. P. Huybers and E. Tziperman (2025) On the Attribution of Weather Events to Climate Change Using Empirically Fit Extreme Value Distributions. *Journal of Climate* 38 DOI:10.1175/JCLI-D-23-0542.1.
- Sugiura, K., T. Ohata, and D. Yang, 2006. Catch characteristics of precipitation gauges in high-latitude regions with high winds. *Journal of Hydrometeorology*, 7, 984-994.
- Spencer, R.W. and J.R. Christy (1992). Precision and radiosonde validation of satellite gridpoint temperature anomalies. Part I: MSU Channel 2. *Journal of Climate*, 5(8) 847-857.
- USGCRP, 2023: *Fifth National Climate Assessment*. Crimmins, A.R., C.W. Avery, D.R. Easterling, K.E. Kunkel, B.C. Stewart, and T.K. Maycock, Eds. U.S. Global Change Research Program, Washington DC, USA. <https://doi.org/10.7930/NCA5.2023>.
- van der Wiel, Karin, Sarah B. Kapnick, Gabriel A. Vecchi,, William F Cooke, Thomas L. Delworth, Liwei Jia, Hiroyuki Murakami, Seth Underwood, and Fanrong Zeng (2016) The Resolution Dependence of Contiguous U.S. Precipitation Extremes in Response to CO2 Forcing. *Journal of Climate* Volume 29 October 2016, <https://doi.org/10.1175/JCLI-D-16-0307.1>
- Vogelsang, T.J. and Franses, P. H. (2005) Testing for Common Deterministic Trend Slopes, *Journal of Econometrics* 126 <https://doi.org/10.1016/j.jeconom.2004.02.004>.

Funding Declaration

JC acknowledges US Department of Energy grant DE-SC0023332.

Competing interests

RM is an unpaid Senior Fellow of the Fraser Institute and an unpaid member of the Academic Advisory Council of the Global Warming Policy Foundation and has provided paid or unpaid advisory services to private sector entities in the law, manufacturing, communications and technology sectors. None of these entities had any knowledge of, involvement with or input into this research.